

Title: Structural connectivity between brainstem nuclei and cerebellum using 7 Tesla MRI in living humans (a pilot study).

Authors: Juan Rodrigo Guerrero Morales¹, Kavita Singh^{2,3}, Marta Biancardi³, María Guadalupe García Gomar^{1,3}.

Affiliations:¹Escuela Nacional de Estudios Superiores Unidad Juriquilla, Universidad Nacional Autónoma de México, ²Multiscale Imaging and Integrative Biophysics Unit, LBN, National Institute on Aging, NIH, Baltimore, MD, USA, ³Brainstem Imaging Laboratory, Department of Radiology, Athinoula A. Martinos Center for Biomedical Imaging, Massachusetts General Hospital and Harvard Medical School

Objective: Investigate the underlying connectivity between motor and arousal brainstem nuclei and cerebellum areas using 7 Tesla Magnetic Resonance Imaging (MRI) and graph theory.

Methods: 7 Tesla MRI (Magnetom; Siemens Healthineers) was performed in one subject using a custom-built 32 channel receive and volume transmit coil¹. The protocol was approved by the Institutional Review Board at the Massachusetts General Hospital and the subject provided written informed consent in accordance with the declaration of Helsinki.

A T_1 -weighted multi-echo magnetization prepared-rapid gradient echo (MEMPRAGE) was acquired with the following parameters echo times (TEs)/repetition time (TR) = [2.39, 5.62]ms/2.53s, inversion time = 1.1s ms, flip angle = 7°, GRAPPA factor = 2, isotropic spatial resolution voxel size = 0.75 mm, field of view = 240 x 240 x 240 mm, acquisition time = 6'34".

Diffusion weighted images (DWI) were acquired with the following parameters: unipolar diffusion-weighting gradients, $b = 2500 \text{ s/mm}^2$ with 60 different directions, TE/TR = 66.8 ms/ 7.4 ms, isotropic voxel size of 1.7 mm³, number of slices = 82, phase encoding direction = anterior/posterior, bandwidth = 1,456 Hz/pixel, partial Fourier = 6/8, acquisition time = 8'53". To perform distortion correction, we acquired seven images with $b = \sim 0 \text{ s/mm}^2$ and opposite phase-encoding direction (posterior/anterior)..

MRI data preprocessing: For the anatomical T_1 -weighted image we computed the root-mean-square of the MEMPRAGE image across echo times. We then rotated it to standard orientation ("RPI"), performed bias field correction using non-uniform intensity normalization (N4ITK)^{2,3}, extracted the brain (FSL-BET) and cropped the lower slices (FSLROI in FSL 5.0.7 tools-FMRIB Software Library, FSL, Oxford, UK). The bias field corrected T_1 -weighted image was then registered to standard MNI space using a non-linear registration (FSL, FLIRT)^{4,5}.

DWI were denoised using local-PCA⁶, motion and distortion corrected (FSL, topup/eddy). We performed probabilistic tractography using the MRtrix3 software package (<http://www.mrtrix.org>). Using dwi2response⁷, we estimated response functions from the preprocessed diffusion-weighted images. These were then used to estimate FOD based on constrained spherical deconvolution using dwi2fod⁸.

To calculate the connectivity between brainstem nuclei and cerebellar areas we used the probabilistic atlas labels of 19 brainstem regions involved in motor and arousal functions in MNI space^{9,10} (<https://www.nitrc.org/projects/brainstemnavig/>), the labels were binarized and transformed using the inverse matrix to T_1 -weighted subject space. Diedrichsen's et al.^{11,12} probabilistic atlas labels in MNI space were used to obtain cerebellar segmentation of 34 areas (shown in figure 1). All labels were used both as seeds and ~~include~~ masks (targets); each tractogram generated and selected a maximum of 250 streamlines with an angle of 85° to connect seeds and targets.

The T_1 -weighted bias field corrected image was then registered to a Power Anisotropy Map derived from the subject DWI using ANTs. The resultant transformation matrix was used to transform all brainstem and cerebellum labels to diffusion space.

To assess the connectivity properties between these brainstem and cerebellar areas each label was defined as a node in an adjacency matrix. After running seed based Constrained Spherical Deconvolution probabilistic tractography⁸ we achieved a 53x53 directional and weighted adjacency matrix.

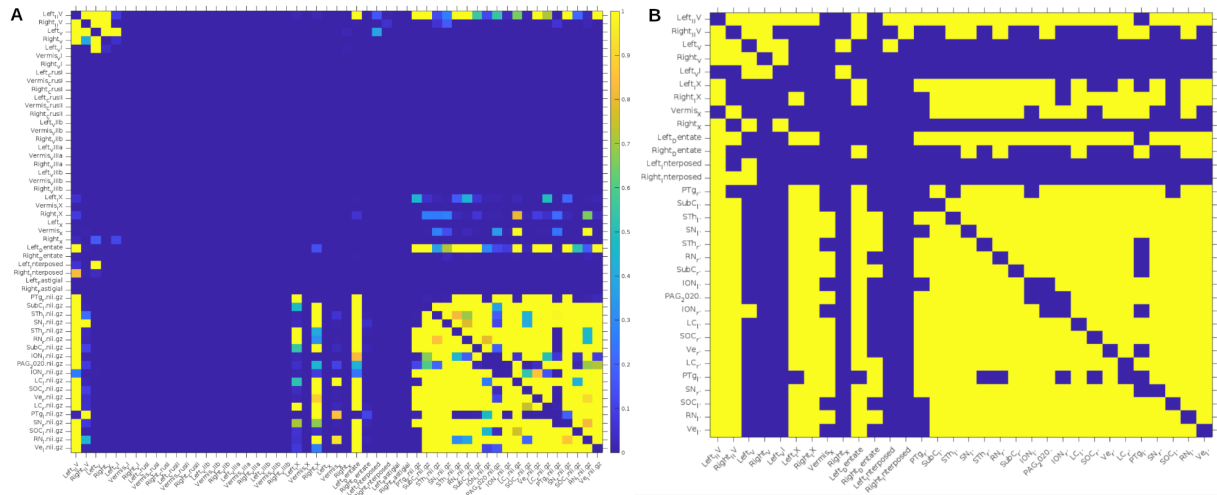


Figure 1. A) Structural connectivity matrix of 34 cerebellar areas and 19 motor and arousal brainstem nuclei. B) Binarized structural connectivity matrix of cerebellar areas and brainstem nuclei nodes that showed connectivity among them ($p = \text{ot threshold} =$). The cerebellum areas correspond to the same nomenclature used in Diedrichsen et al., 2009^{11,12}. PTg: pedunculotegmental nucleus, SubC: subcoeruleus, Sth: subthalamic nucleus, SN: substantia nigra, RN: red nucleus, ION: inferior olivary nucleus, PAG: periaqueductal gray, SOC: superior olivary complex, Ve: vestibular nuclei complex, LC: locus coeruleus.

Graph Theory: The adjacency matrix was then binarized and reduced to include only the nodes that did show connection with other nodes. This yielded a 32 by 32 matrix with 13 cerebellum areas and 19 brainstem areas (Figure 1B). Node degree and closeness were calculated, the degree of a node tells us how many connections are made with other nodes, therefore it is a direct measure of structural connectivity between brainstem and cerebellum areas. Closeness is a centrality measure, a central node is of functional importance because it receives high loads of information, and thus, links several other nodes together. A node with a high closeness centrality is one that connects directly (short distances) with other nodes; this behavior is observed in motor and sensory areas of the central nervous system. Finally, following Sporns¹³ and Humphires et.,al.¹⁴, network topology was investigated using the small-world index σ .

Results: Our adjacency matrix (Figure 1A) shows that deep cerebellar nuclei are strongly connected to the brainstem and presents an small world index $\sigma = 1.48676$, consistent with a small-world graph and. Left_IIV showed greater closeness, which is a centrality measure, a central vertex is of functional importance receiving high loads of information and linking several other areas together (Figure 2A). Left_I_IV showed greater connectivity (degree) which is a direct measure of structural connectivity (Figure 2B).

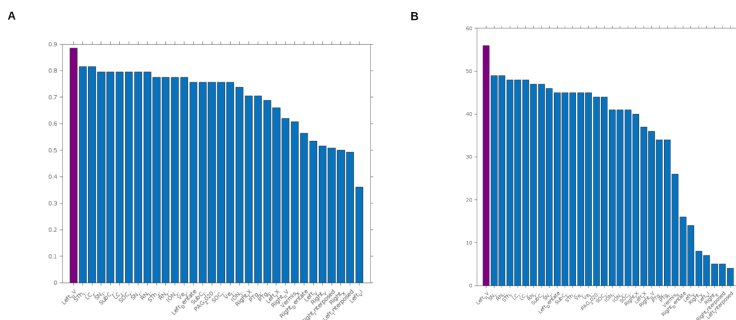


Figure 2. A) Centrality calculated for cerebellum areas and brainstem nuclei. B) Degree calculated for cerebellum areas and brainstem nuclei (nuclei acronyms as in Figure 1).

Conclusion: This study provides insights about the close interrelationship between cerebellar lobes, cerebellar deep nuclei and brainstem nuclei using non-invasive tools such as 7 Tesla high-resolution MRI for mapping the structural connections among

these structures. These findings might be useful to further understand physiology and neuropathology associated with these structures.

References:

1. Keil, B., Triantafyllou, C., Hamm, M. & Wald, L. L. Design Optimization of a 32-Channel Head Coil at 7 T. in (2009).
2. Avants, B. B. *et al.* A reproducible evaluation of ANTs similarity metric performance in brain image registration. *NeuroImage* **54**, 2033–2044 (2011).
3. Tustison, N. J. *et al.* N4ITK: Improved N3 Bias Correction. *IEEE Trans. Med. Imaging* **29**, 1310–1320 (2010).
4. Smith, S. M. *et al.* Advances in functional and structural MR image analysis and implementation as FSL. *NeuroImage* **23**, S208–S219 (2004).
5. Andersson, J. L. R., Skare, S. & Ashburner, J. How to correct susceptibility distortions in spin-echo echo-planar images: application to diffusion tensor imaging. *NeuroImage* **20**, 870–888 (2003).
6. Manjón, J. V. *et al.* Diffusion Weighted Image Denoising Using Overcomplete Local PCA. *PLoS ONE* **8**, e73021 (2013).
7. Smith, R. E., Tournier, J.-D., Calamante, F. & Connelly, A. SIFT: Spherical-deconvolution informed filtering of tractograms. *NeuroImage* **67**, 298–312 (2013).
8. Tournier, J.-D., Calamante, F. & Connelly, A. Robust determination of the fibre orientation distribution in diffusion MRI: Non-negativity constrained super-resolved spherical deconvolution. *NeuroImage* **35**, 1459–1472 (2007).
9. Bianciardi, M. *et al.* In vivo functional connectome of human brainstem nuclei of the ascending arousal, autonomic, and motor systems by high spatial resolution 7-Tesla fMRI. *Magn. Reson. Mater. Phys. Biol. Med.* **29**, 451–462 (2016).
10. Bianciardi, M. *et al.* Toward an *In Vivo* Neuroimaging Template of Human Brainstem Nuclei of the Ascending Arousal, Autonomic, and Motor Systems. *Brain Connect.* **5**, 597–607 (2015).
11. Diedrichsen, J., Balsters, J. H., Flavell, J., Cussans, E. & Ramnani, N. A probabilistic MR atlas of the human cerebellum. *NeuroImage* **46**, 39–46 (2009).
12. Diedrichsen, J. *et al.* Imaging the deep cerebellar nuclei: A probabilistic atlas and normalization procedure. *NeuroImage* **54**, 1786–1794 (2011).
13. Sporns, O., Honey, C. J. & Kötter, R. Identification and Classification of Hubs in Brain Networks. *PLoS ONE* **2**, e1049 (2007).
14. Humphries, M. D., Gurney, K. & Prescott, T. J. The brainstem reticular formation is a small-world, not scale-free, network. *Proc. Biol. Sci.* **273**, 503–511 (2006).